Feeding Behavior Modifies the Circadian Variation in RR and QT intervals by Distinct Mechanisms in Mice.

Makoto Ono[1], Don E. Burgess[1], Sidney R. Johnson[1], Claude S. Elayi[2], Karyn A. Esser[3], Tanya S. Seward[1], Carie R. Boychuk[4], Andrés P. Carreño[1], Rebecca A. Stalcup[1], Abhilash Prabhat[1], Elizabeth A. Schroder[1,5*], Brian P. Delisle[1*]

[1]Department of Physiology, University of Kentucky, Lexington, KY, USA
[2]CHI Saint Joseph Hospital, Lexington, KY, USA
[3]University of Florida, Gainesville, FL, USA
[4]Dalton Cardiovascular Research Center, Department of Biomedical Sciences, University of Missouri, Columbia, MO, USA
[5]Department of Internal Medicine, University of Kentucky, Lexington, KY, USA

*Contributed equally to the study

Running Title: Shaping 24-hour Rhythms in RR and QT Intervals

Corresponding authors:

Elizabeth A. Schroder
Department of Internal Medicine
859-323-5571
eschr0@uky.edu
780 Rose Street, Medical Science Building, Rm: MN-512, Lexington, KY 40536-0298

Brian P. Delisle
(859) 323-2797
brian.delisle@uky.edu
741 S Limestone Street BBSRB B353, Lexington, KY, 40536

Word Count: 7,974

Key Words: Cardiac Electrophysiology**,** Time of Feeding**,** Core Body Temperature**,** Circadian Rhythms**,** Autonomic Nervous System

Abstract

Rhythmic feeding behavior is critical for regulating the phase and amplitude in the ≈24-hour variation of the heart rate (RR intervals), ventricular repolarization (QT intervals), and core body temperature in mice. We hypothesized the changes in cardiac electrophysiology associated with feeding behavior were secondary to changes in core body temperature. Telemetry was used to record electrocardiograms and core body temperature in mice during ad libitum-fed conditions and after inverting normal feeding behavior by restricting food access to the light cycle. Light cycle-restricted feeding quickly modified the phase and amplitude of the 24-hour rhythms in RR intervals, QT intervals, and core body temperature to realign with the new feeding time. Heart rate variability analysis and inhibiting β-adrenergic and muscarinic receptors suggested that the changes in the phase and amplitude of the 24-hour rhythms in RR intervals were secondary to changes in autonomic signaling. In contrast, the changes in the QT intervals closely mirrored changes in core body temperature. Studies at thermoneutrality confirmed the daily variation in the QT interval, but not the RR interval, and reflected daily changes in core body temperature (even in ad libitum-fed conditions). Correcting the QT interval for differences in core body temperature helped to unmask QT interval prolongation after starting light cycle-restricted feeding and in a mouse model of long QT syndrome. We conclude feeding behavior alters autonomic signaling and core body temperature to regulate the phase and amplitude in RR and QT intervals, respectively.

Abbreviations:

ECG - Electrocardiogram
pHF - high-frequency power
pLF - low-frequency power
SD - standard deviation
WT - Wild type
$QT_{37°C}$ - QT corrected to 37°C
ZT - Zeitgeber Time

New and Noteworthy: We used time-restricted feeding and thermoneutrality to demonstrate that different mechanisms regulate the 24-hour rhythms in heart rate and ventricular repolarization. The daily rhythm in heart rate reflects changes in autonomic input, whereas daily rhythms in ventricular repolarization reflect changes in core body temperature. This novel finding has major implications for understanding 24-hour rhythms in mouse cardiac electrophysiology, arrhythmia susceptibility in transgenic mouse models, and interpretability of cardiac electrophysiological data acquired in thermoneutrality.

Introduction

Organisms have evolved circadian rhythms in physiology to anticipate changes during the 24 hours in the external environment.(1) In mammals, circadian rhythms are generated at the cellular level by the circadian clock mechanism, a transcription-translation feedback loop that cycles with a periodicity of ≈24 hours.(2, 3) The circadian clock mechanism in the suprachiasmatic nucleus (SCN) of the hypothalamus entrains to the light cycle, and light-entrained SCN neurons signal to neighboring SCN neurons and other brain nuclei to align neurohumoral signaling, behavioral rhythms, and peripheral circadian clocks throughout the body.(4, 5) Several studies suggest SCN signaling modifies autonomic input to the heart to generate circadian variations in cardiac electrophysiology (i.e., RR and QT intervals).(6, 7) Studies also show that the circadian clock mechanism in cardiomyocytes contributes to 24-hour rhythms in the RR and QT intervals by altering the expression of genes, proteins, and different cardiac ionic currents.(8-14)

Feeding behavior is an important timekeeping cue for aligning circadian clocks in peripheral tissues, including the heart. Mouse studies reveal that restricting feeding to the inverse time of normal feeding behavior (i.e., light cycle-restricted feeding) realigns the phase of circadian mRNA expression in the heart and 24-hour rhythms in cardiac electrophysiology to the new feeding behavior.(15, 16) The effect of light cycle-restricted feeding on the realignment of 24-hour rhythms in cardiac electrophysiology is not secondary to changes in the circadian clocks in the SCN or cardiomyocytes. The reason is the circadian clock in the SCN remains entrained to the light cycle during light cycle-restricted feeding(17), and genetic disruption of the cardiomyocyte circadian clock by inducing deletion of BMAL1 does not prevent realignment of 24-hour rhythms in cardiac electrophysiology with feeding.(18) This study determined how feeding behavior impacts 24-hour rhythms in the phase and amplitude of the RR and QT intervals in mice.

Several studies have demonstrated a strong temperature dependence in the RR and QT interval.(19-29) In addition, previous studies have shown that light cycle-restricted feeding in mice alters the phase and amplitude of the 24-hour rhythm in core body temperature.(17, 30) This raises the intriguing possibility that feeding modifies 24-hour cardiac electrophysiology rhythms by altering core body temperature rhythms.

In this study, we tested whether light-cycle restricted feeding similarly altered the phase and amplitudes of the 24-hour rhythms of the RR intervals, QT intervals, and core body temperature. We found that the changes in the 24-hour rhythm of the RR interval during light cycle-restricted feeding were only partially explained by changes in the core body temperature, and pharmacological studies showed the 24-hour rhythm in the RR interval was strongly influenced by autonomic signaling. In contrast, the changes in the 24-hour rhythm in the QT interval during light cycle-restricted feeding closely mirrored changes in the core body temperature. Correcting the QT interval for core body temperature was important in identifying abnormal changes in the QT interval in transgenic mouse models of long QT syndrome. We conclude that feeding behavior aligns the 24-hour rhythms in the RR and QT intervals by distinct mechanisms in mice.

Methods

Animals. The mice used in this study were male on the 129S6 background strain. The 129S6 mouse strain has been previously characterized in the ΔKPQ mouse model (*Scn5a*$^{+/\Delta KPQ}$ mice).(31, 32) For studies comparing the genotype-specific differences, age-matched (wild type, WT) and *Scn5a*$^{+/\Delta KPQ}$ littermates were used. Mice were fed Teklad Global 18% protein rodent diet (2018). All procedures complied with the Association for Assessment and Accreditation of Laboratory Animal Care guidelines and were approved by the Institutional Animal Care and Use Committee at the University of Kentucky. Dr. Peter Carmeliet kindly provided the *Scn5a*$^{+/\Delta KPQ}$ mouse strain.(33) This study represents new and re-analysis of data collected previously.(15) All studies were performed at room temperature (23 ± 2°C) except for data presented in **Figure 7**. These studies were done in mice housed in thermoneutral temperatures (30 ± 2°C).(34) After the study, mice were euthanized by anesthetic overdose followed by cervical dislocation.

Telemetry. We used telemetry to measure electrocardiogram (ECG), core body temperature, and locomotor activity. Mice were anesthetized with isoflurane (2-4%) using a nose cone attached to an anesthetic gas vaporizer and implanted with PhysioTel ETA-F10 (Data Sciences International) telemetry transmitter units. ECG telemetry data were recorded at 1000 Hz, and RR, QT, and PR interval analyses were done using MATLAB (MathWorks), similar to those previously described.(8, 15, 18) ECG traces recorded for each hour were aligned to the peak of the R wave to generate an ensemble ECG trace. The beginning of the P wave was defined as the point where the slope of the P wave profile changed by more than 0.001 mV/ms; the Q wave was defined as the point where the slope of the profile changed from negative to positive at the base of the QRS complex; the end of the T wave was defined as the point of intersection of T wave maximum slope with baseline.(35)

Statistical analysis. For some graphs, data are shown as the mean and standard deviation of the mean (SD). For other graphs, a data point for each animal is shown with a horizontal bar at the mean. The statistical JTK_CYCLE package confirmed significant cyclical rhythms at $p<0.05$ before analyzing the data using cosine waveform curve fitting.(36). Data were analyzed in PRISM (GraphPad). Details of statistical analyses for each experiment are reported in the figure legends.

Results

Experiment 1: Determine how long it takes for light cycle-restricted feeding to alter the 24-hour rhythms in cardiac electrophysiology and core body temperature.

Three to four-month-old WT mice housed in 12-hour light/dark cycles at room temperature with ad libitum access to water were used in this study. To initiate light cycle-restricted feeding, food was removed at 9 h after the beginning of the light cycle (Zeitgeber time or ZT = 9). The next day, food presentation was restricted to 7 h during the light cycle, between ZT 2–9 for two weeks. Light cycle-restricted feeding caused mice to lose body mass during the first week (**Figure S1**). However, caloric intake increased after that, and similar to previous reports, light cycle-restricted-fed animals re-gained body mass after two weeks.(37)

We used *in vivo* telemetry to longitudinally record electrocardiogram (ECG) data from mice before and after switching to light cycle-restricted feeding (**Figure 1A**). Data recorded shortly after starting light cycle-restricted feeding revealed immediate impacts on cardiac electrophysiology. Data recorded two weeks after beginning light cycle-restricted feeding indicated the steady state changes.(17) The top, left panel in **Figure 1B** shows a three-day time series for changes in the hourly mean heart rate (RR interval), the duration of ventricular repolarization (QT interval), and the duration of atrial to ventricular conduction (PR interval) in ad libitum-fed conditions. The time series showed that the amplitude in the daily rhythms in RR, QT, and PR intervals peaked at a similar time (i.e., had similar acrophases) during the light cycle. However, a new 24-hour rhythm in the ECG data emerged one day after starting light cycle-restricted feeding. The new 24-hour rhythms had larger amplitudes and peaked in the dark cycle. The changed 24-hour rhythms in the ECG data after starting light cycle-restricted feeding were not transitory and persisted for two weeks.

Previous studies show that light cycle-restricted feeding causes analogous changes in daily core body temperature rhythms.(17, 38) We found that light cycle-restricted feeding changed the daily core body temperature rhythm in a way that largely mirrored the changes in the daily rhythms in RR, QT, and PR intervals (**Figure 1B**).

We quantified the changes in the 24-hour rhythms in cardiac electrophysiology and core body temperature before and after starting light cycle-restricted feeding. Almost all of the individual ECG and core body temperature time series recorded from ad libitum-fed mice, one day after starting light cycle-restricted feeding, and two weeks after starting light cycle-restricted feeding had significant cyclical rhythms with a periodicity of ≈24 hours (i.e, JTK analysis showed $p<0.05$) (see **Supplemental Table 1**).

The hourly mean data for RR, QT, and PR intervals and core body temperature for each mouse were fit with the cosine curve function:

$$\text{Interval} = A*\cos[2\pi*t/T - \emptyset] + m$$

to calculate the period (T), the time between the peak amplitudes; acrophase (∅), the phase of the peak amplitude in relation to the start of the light cycle (ZT = 0); the amplitude (A), one-half of the peak to trough; and the mesor (m), the rhythm adjusted mean (calculated data are presented in **Supplement Table 1**).(8, 15, 18)

Data showed that light cycle-restricted feeding caused large changes in the acrophase, amplitude, and mesor of daily rhythms in RR intervals, QT intervals, PR intervals, and core body temperature (**Figures 2A, 2B**). No or very small additional changes were seen in the cyclical ECG and core body temperature rhythms two weeks after starting light cycle-restricted feeding.

We conclude only one day of light cycle-restricted feeding causes large, simultaneous, and abrupt changes in the phase, amplitude, and mesor in the ≈24-hour rhythms of cardiac electrophysiology and core body temperature.

Experiment 2: Light cycle-restricted feeding impacts the 24-hour rhythm in the RR interval by modifying core body temperature and autonomic input to the heart.

We first estimated how much of the 24-hour rhythm in the RR interval is expected to be driven by daily change in core body temperature ($RR_{\text{core body temperature}}$ interval). We used a Q_{10} value based on the Q_{10} value reported in isolated WT mouse hearts.(23) For the $RR_{\text{core body temperature}}$ interval calculation, we used a reference core body temperature of 37°C and an RR interval of 116 ms because these were the mean values in WT mice in ad libitum-fed conditions.

$$RR_{\text{core body temperature}} \text{ interval} = 116 \text{ ms} * (0.40)^{((\text{core body temperature}-37.0)/10)}$$

We directly compared the estimated $RR_{\text{core body temperature}}$ interval with the RR interval measured from WT mice in ad libitum-fed conditions, immediately after starting light cycle-restricted feeding, and two weeks after starting light cycle-restricted feeding (**Figure 3**). The data suggest that the $RR_{\text{core body temperature}}$ interval represented a significant portion of the amplitude in the RR interval during ad libitum-fed conditions. However, a large difference between the $RR_{\text{core body temperature}}$ and RR interval emerged during the dark cycle one day after starting light cycle-restricted feeding (**Figure 3A**), suggesting that additional factors contributed to the amplitude of the 24-hour rhythm in RR intervals one day after starting light cycle-restricted feeding.

The 24-hour rhythm in the RR interval is classically thought to reflect changes in autonomic input to the heart and activity.(6, 39, 40) We quantified changes in autonomic input to the heart by measuring changes in the heart rate variability from mice in ad libitum-fed conditions and after switching to light cycle-restricted feeding. We followed the approaches outlined by Fenske et al. (41). Interpolated RR interval time series were generated for spectral analysis and determination of frequency domain components for heart rate variability analyses. In mice, the frequency range to classify the high-frequency (HF) component is 1.5-4.0 Hz, and the frequency range used to classify the low-frequency (LF) component is 0.4-1.5 Hz (41) The HF component is generally accepted to correspond to the parasympathetic outflow related to respiratory sinus arrhythmia, and the LF component is thought to primarily reflect autonomic outflow associated with the baroreceptor reflex.(42)

Power Spectral Density $\mathcal{P}(f)$ has units of power per frequency (ms^2/Hz). The HF and LF components represent the power within a frequency band and are related to the integration:

$$P_{band} = \int_{f_1}^{f_2} \mathcal{P}(f) df$$

The units of the differential cancel the frequency units, so the units for the HF and LF components are in ms^2. Normalization is based on the discrete version of Parseval's theorem. It allows us to consistently approximate the integration for LF and HF components of the variance for the underlying RR time series.(43)

In ad libitum-fed conditions, the mean HF component was higher during the light cycle than the dark cycle. One day after starting light cycle-restricted feeding, the mean HF component increased during the dark cycle, and this persisted two weeks after

starting light cycle-restricted feeding (**Figure 3A, 3B**). Similar trends were seen for the LF component but did not reach statistical significance (**Figure 3S**).

In ad libitum-fed conditions, the mean activity was lower during the light cycle than the dark cycle. This trend persisted initially after starting light cycle-restricted feeding, but the difference between the light and dark cycle activity levels disappeared after two weeks.

The individual mouse three-day time series data for the HF and activity components did not show significant cyclical rhythms for most mice (JTK analysis P>0.05), and the data were not well described using cosine waveform curve fitting. Therefore, we analyzed the relative rhythmicity between the RR interval and the HF component or activity using cross-correlation analyses.(44) As part of the analysis, we included the cross-correlation between RR interval and core body temperature. We used the R function "ccf" to calculate the cross-correlation.(45) The formula used in "ccf" to calculate the cross-correlation between two time series $X(t), Y(t)$ has the form

$$c_{xy}(t) = \frac{1}{n} \sum_{s=\max(1,-t)}^{\min(n-t,n)} [X(s+t) - \bar{X}]\,[Y(s+t) - \bar{Y}]\,,\ r_{xy}(t) = \frac{c_{xy}(t)}{c_{xy}(0)}$$

Figure 4 shows the cross-correlation for RR-core body temperature, RR-HF, and RR-activity from mice in ad libitum-fed conditions and after starting light cycle-restricted feeding. The cross-correlation between the RR-core body temperature and RR-HF showed strongly correlated rhythmicity that peaked at a lag of 0 in all three conditions, but the RR-activity cross-correlation only showed correlated rhythmicity in ad libitum-fed conditions. The data suggested that altered autonomic signaling and not activity may be important for modifying the daily rhythm in the RR interval during light cycle-restricted feeding.

We directly tested the involvement of autonomic signaling by doing intraperitoneal injections of propranolol hydrochloride and atropine sulfate (10 mg/kg each) in six to eight-month-old telemetered WT mice undergoing light cycle-restricted feeding.(46-48) Propranolol and atropine inhibit β-adrenergic and muscarinic receptor activation, respectively. We injected the mice at ZT 23.5 (when the daily rhythm in the RR interval peaked) and 9.5 (when the RR interval was at its nadir) for two consecutive days. The feeding onset was delayed one hour to ZT 3 to separate the food anticipatory decrease in RR interval from the start of the light cycle. Propranolol and atropine injections caused a loss in the 24-hour rhythms of the RR interval, core body temperature, and the difference between the $RR_{\text{core body temperature}}$ interval and RR interval (**Figure 5A, 5B, and 5C**).

These data suggest light cycle-restricted feeding modifies the 24-hour rhythm in the RR interval by altering core body temperature and autonomic input to the heart.

Experiment 3: The 24-hour rhythm in the QT interval during light cycle-restricted feeding primarily reflects changes in the core body temperature.

The time series data shows that longitudinal changes in the hourly mean QT interval occur in parallel to the changes in the RR interval and mirror changes in core body temperature (**Figure 1**). The duration of the QT interval in mice is thought to be independent of the RR interval.(9, 49-51) Therefore, we quantified the relation between the QT interval and core body temperature. We used an approach similar to that described previously to correct the heart rate corrected QT interval to core body temperature in beagles.(29) The hourly mean QT intervals were plotted against the corresponding core body temperature for all data collected in ad libitum- and light cycle-restricted fed mice, and we identified a strong negative linear relationship between the mean QT interval and core body temperature (**Figure 6A**).(29) The average slope of the linear QT-core body temperature relation was used to derive a QT-core body temperature correction formula. We corrected the QT intervals to 37°C ($QT_{37°C}$ interval) because 37°C was the daily mean in the core body temperature for ad libitum-fed mice.

$$QT_{37°C} = \text{QT interval}-(4.3*(37°C\text{-core body temperature}))$$

Correcting the time series of the 24-hour rhythm in the QT interval for core body temperature caused a loss in the 24-hour rhythm in the QT interval for mice in ad libitum and light cycle-restricted feeding (**Figure 6B**).

We confirmed the 24-hour rhythm in the QT interval reflected changes in core body temperature (and not the RR interval) by studying the ECG properties of the mice housed in thermoneutrality under ad libitum-fed conditions. Studying mice in thermoneutrality alters autonomic tone to dramatically slow the basal heart rate without causing large changes in the daily rhythm of the core body temperature.(52) Housing mice at thermoneutrality slowed the RR interval and generated a large difference in the $RR_{\text{core body temperature}}$ not seen in ad libitum-fed mice housed at room temperature (compare **Figure 3, top left panel** to **Figure 7A**). In contrast, both the QT and $QT_{37°C}$ intervals measured in thermoneutrality were qualitatively similar to the QT and $QT_{37°C}$ intervals measured at room temperature (compare **Figure 6B**, **left panel** to **Figure 7A**). The $QT_{37°C}$ interval in mice housed at thermoneutrality also generated a horizontal line when plotted as a function of core body temperature (**Figure 7B**). We plotted the hourly mean QT intervals against the corresponding core body temperature. The negative linear relationship between the mean QT interval and core body temperature was similar to mice housed at room temperature (compare **Figure 6A and 7C**).(29)

These data support the concept that the 24-hour rhythms in the RR and QT intervals are regulated by distinct mechanisms- even in ad libitum fed mice. Specifically, the 24-hour rhythm of the RR interval is sensitive to changes in core body temperature and autonomic signaling, whereas the 24-hour rhythm of the QT interval primarily reflects changes in the core body temperature.

Experiment 4: Determine the impact of core body temperature on the QT interval in a transgenic mouse model of long QT syndrome.

We previously showed that light cycle-restricted feeding for two weeks prolonged the RR and QT intervals in *Scn5a*$^{+/\Delta KPQ}$ mice. However, the QT intervals in this study were not corrected for core body temperature.(15) We quantified the ECG properties and core body temperature measured in *Scn5a*$^{+/\Delta KPQ}$ mice during ad libitum-fed conditions

and after starting light cycle-restricted feeding. The changes in the 24-hour rhythm of RR interval, QT interval, PR interval, and core body temperature were similar to those recorded in WT mice (**Figures 1 and 3S**). Cosine fitting analysis of ECG data from the *Scn5a*$^{+/\Delta KPQ}$ mice showed that, one day after starting light cycle-restricted feeding, there was an immediate change in the phase, increase in amplitude, and change in the mesor for 24-hour rhythms in the RR intervals, QT intervals, PR intervals, and core body temperature (**Figure 4S**). We compared the $QT_{37°C}$ interval for WT and *Scn5a*$^{+/\Delta KPQ}$ mice in ad libitum-fed conditions and after starting light cycle-restricted feeding (**Figure 8A**). The $QT_{37°C}$ interval was not different between WT and *Scn5a*$^{+/\Delta KPQ}$ mice in ad libitum-fed conditions (**Figure 8B**). After starting light cycle-restricted feeding, the $QT_{37°C}$ interval became longer in WT and *Scn5a*$^{+/\Delta KPQ}$ mice. Light cycle-restricted feeding also unmasked a genotype-specific difference in $QT_{37°C}$ intervals measured from WT and *Scn5a*$^{+/\Delta KPQ}$ mice (**Figure 8B**).

Discussion

We determined the mechanisms that underlie the changes in the 24-hour rhythms of the RR and QT intervals during light cycle-restricted feeding. We found that one day after starting light cycle-restricted feeding, the 24-hour rhythms in the RR intervals, QT intervals, PR intervals, and core body temperature changed to a new phase with a larger amplitude (**Figures 1B, 2A, 2B**). The Changes in the 24-hour rhythm of the RR interval correlated with changes in heart rate variability (**Figures 3, 4**), and inhibiting β-adrenergic and muscarinic receptor activation in light cycle restricted-fed mice caused a loss in the 24-hour rhythm of the RR interval (**Figure 5**). The 24-hour rhythm in the QT interval showed a strong linear relation with core body temperature (**Figure 6**), and studies in ad libitum-fed mice housed in thermoneutrality confirmed that the 24-hour rhythm in the QT interval primarily reflected changes in core body temperature (not the RR interval) (**Figure 7**). Correcting the QT interval for core body temperature allowed us to identify abnormal QT interval prolongation in a transgenic mouse model of long QT syndrome (**Figure 8**).

Feeding behavior impacts the 24-hour rhythm in the RR interval (heart rate) by modifying autonomic input to the heart.

Studies suggested that the circadian clock in the SCN modified autonomic signaling to generate the 24-hour rhythm in heart rate.(6, 53-56) These studies were supported by data showing that ablation of the SCN or transgenic mice lacking the core circadian clock transcription factor *Bmal1* (e.g., *Bmal1*$^{-/-}$) did not have a 24-hour rhythm in heart rate.(57-59) Light cycle-restricted feeding is not thought to impact the phase of the circadian clock mechanism in the SCN;(17) therefore, it was surprising that light cycle-restricted feeding caused a significant phase shift in the 24-hour rhythm of heart rate.(15) Light cycle-restricted feeding in mice also shifts the phase of circadian gene expression in peripheral tissues, including the heart, to align with the timing of feeding behavior.(17) Several studies implicate the cardiomyocyte circadian clock in regulating gene expression essential for cardiac excitability, cardiac electrophysiology, and heart rate.(8-12, 58, 60) One might predict that light cycle-restricted feeding shifts the phase of cardiomyocyte gene expression to facilitate changes in 24-hour rhythms of heart rate. However, genetically disrupting the cardiomyocyte-specific circadian clock (by inducing

the deletion of *Bmal1*) did not abolish the light cycle-restricted feeding-mediated phase shift in the 24-hour rhythm in heart rate.(18) We conclude that autonomic receptor-mediated signaling largely shapes the 24-hour rhythm in heart rate during light cycle-restricted feeding.

The 24-hour rhythm in the QT depends on core body temperature.

We now report a robust linear QT-core body temperature relation in mice, and correcting the QT interval for core body temperature caused a loss in the 24-hour rhythm of the QT interval. These new data suggest the changes in the 24-hour rhythm of the QT interval in mice during light cycle-restricted feeding primarily reflect daily changes in core body temperature (not the RR interval). The idea that the 24-hour rhythm in the QT interval in mice primarily reflects core body temperature is also supported by a study showing that the 24-hour rhythm of the QT interval in mice is independent of the RR interval.(9) core body temperature was not reported in the study, but the observed change in the amplitude of the daily rhythm in the QT interval (4-5 ms) is consistent with a core body temperature amplitude typically seen in mice (1°C).(61)

The QT interval is used clinically in humans to assess the risk for certain deadly ventricular arrhythmias.(62) We extended our light cycle-restricted feeding studies to quantify changes in the QT interval in a transgenic knock-in mouse model that expresses a mutation linked to long QT syndrome in people.(33) Correcting the QT interval for core body temperature allowed direct comparisons of QT intervals at different core body temperatures across the 24-hour cycle, identified genotype-specific differences in the QT interval independent of core body temperature, and showed that light cycle-restricted feeding caused a prolongation of the QT interval in WT and *Scn5a*$^{+/\Delta KPQ}$ mice. These studies underscore the importance of monitoring and considering the influence of core body temperature when measuring QT intervals.

An important question is whether these data may be clinically relevant to humans. We propose that the daily rhythm in core body temperature also contributes to the 24-hour rhythm in the heart rate corrected QT (QTc) interval observed in people. Several studies report a temperature dependence of the QTc interval in people is 10-15 ms for every 1°C change in core body temperature.(24-29) The peak-to-trough amplitude in the daily core body temperature rhythm in people is about 1°C, and the peak-to-trough amplitude in the 24-hour rhythm in the QTc interval is 10-20 ms.(63, 64) Future studies that measure the QT interval and core body temperature across the 24-hour cycle in people will help delineate how much of the 24-hour rhythms in the QTc interval reflect temperature-dependent changes in the properties of ventricular repolarization. Consideration of the influence of core body temperature on the QTc interval is warranted when the core body temperature might be different due to physiological, behavioral, environmental, or pharmacological changes (for example, patients with hypothermia or sepsis).

Implications

Modern lifestyles disrupt evolutionarily conserved behavioral and environmental timekeeping cues critical for maintaining healthy circadian homeostatic mechanisms.(65) Our findings suggest that feeding behavior is a critical timekeeping

cue for daily core body temperature and cardiac electrophysiology rhythms in mice. However, we did not see feeding as being a critical timekeeping cue for activity rhythms. This suggests that eating at an inverse time may cause misalignment between 24-hour rhythms in core body temperature, cardiac electrophysiology, and activity rhythms. If conserved, modern lifestyles that disrupt feeding rhythms in people may negatively impact the alignment between core body temperature, cardiac electrophysiological, and activity rhythms to impair cardiac performance and influence arrhythmogenic risk.

Another implication of this study is that it underscores the importance that daily rhythms in core body temperature have in shaping 24-hour rhythms in ventricular repolarization. Continuous core body temperature monitoring is not routinely performed in people undergoing electrophysiological testing despite its contribution to heart rate and QTc intervals. This is especially true in studies that monitor changes in heart rate and QTc intervals across the 24-hour cycle.

Limitations

Observing a temperature dependence on the QT interval is not necessarily new and has been previously reported.(29) What is new is data suggesting the daily change in core body temperature is primarily responsible for generating a 24-hour rhythm in the QT interval. Ad libitum feeding may not be the best control for restricted light-cycle feeding. A dark cycle-restricted feeding control would rule out any potential effect of food consumption during the light phase seen in ad libitum-fed mice. Fasting mice makes them vulnerable to torpor (a transient hibernating-like state that causes a significant drop in heart rate and core body temperature below 32°C.(22) Our model of light cycle-restricted feeding did not calorically restrict the mice, and the mice continued to eat 3-4 grams of food per day during light cycle-restricted feeding (**Figure 1S**) and gained mass after one week (**Figure 1S**). Another limitation is that this study used only male mice. Results in female mice may differ. The mice used in the pharmacological study were older than those used in the initial light-cycle restricted feeding study. Whether a long $QT_{37°C}$ interval is associated with an increased risk for spontaneous ventricular arrhythmias remains unclear. We found that, during light cycle-restricted feeding, the daily rhythm in the PR interval simultaneously shifted with the RR and QT intervals and core body temperature. However, due to the small absolute amplitude in the PR interval in response to light cycle-restricted feeding, it was difficult to determine if the PR interval reflected core body temperature, autonomic regulation of the heart, or both. The analyses in these studies focused on studying hourly mean values and 24-hour rhythms. We did not quantify the data at higher resolutions or study possible ultradian rhythms. Many cardiac electrophysiological channels that underlie the electrical rhythm of the heart, specifically ventricular repolarization, are not only temperature-sensitive but also time-of-day sensitive. Future studies examining the expression/activity of key components and circadian clock/autonomic nervous system markers in light cycle restricted feeding are warranted. Lastly, caution must be used when extrapolating data from mice to humans.(51, 66)

Summary

Daily rhythms in cardiac electrophysiology align with feeding and activity cycles via signals originating from the SCN. Restricting food availability to the light cycle disrupts

the association between environmental and behavioral timekeeping cues, resulting in the alignment of the daily rhythms of cardiac electrophysiology with the new feeding behavior. The alignment of the 24-hour rhythm in the RR interval primarily reflects changes in autonomic input to the heart. In contrast, the phase of the QT interval mirrors changes in core body temperature. Thermoneutrality studies suggest the distinct regulation of the 24-hour rhythms in RR and QT intervals also occurs in ad libitum-fed mice. We conclude that feeding-induced changes in daily autonomic signaling and core body temperature rhythms facilitate the alignment of 24-hour rhythms in heart rate and ventricular repolarization.

Competing interests

None declared.

Author contributions

All authors contributed to drafting the work and revising it critically for important intellectual content, approved the final version of the manuscript, and qualified for authorship.

Funding

This work was supported by National Heart Lung and Blood Institute grants R01HL153042 and R01HL141343. This publication was supported by the National Center for Research Resources and the National Center for Advancing Translational Sciences, National Institutes of Health, through Grant UL1TR001998**.** The content is solely the responsibility of the authors and does not necessarily represent the official views of the NIH.

Data Availability

Data will be made available upon reasonable request.

Acknowledgment

We want to thank Drs. Wayne Giles and Chao-Yin Chen (University of California, Davis) for providing feedback and discussion. We also acknowledge Isabel Stumpf (Centre College) and David Schneider (Centre College) for technical assistance.

References

1. **Thosar SS, and Shea SA**. Circadian control of human cardiovascular function. *Curr Opin Pharmacol* 57: 89-97, 2021.
2. **Mohawk JA, Green CB, and Takahashi JS**. Central and peripheral circadian clocks in mammals. *Annu Rev Neurosci* 35: 445-462, 2012.
3. **Mohawk JA, and Takahashi JS**. Cell autonomy and synchrony of suprachiasmatic nucleus circadian oscillators. *Trends Neurosci* 34: 349-358, 2011.
4. **Buijs RM, and Kalsbeek A**. Hypothalamic integration of central and peripheral clocks. *Nat Rev Neurosci* 2: 521-526, 2001.
5. **Hastings MH, Maywood ES, and Brancaccio M**. Generation of circadian rhythms in the suprachiasmatic nucleus. *Nat Rev Neurosci* 19: 453-469, 2018.

6. **Tong M, Watanabe E, Yamamoto N, Nagahata-Ishiguro M, Maemura K, Takeda N, Nagai R, and Ozaki Y**. Circadian expressions of cardiac ion channel genes in mouse might be associated with the central clock in the SCN but not the peripheral clock in the heart. *Biol Rhythm Res* 44: 519-530, 2013.

7. **Scheer FA, Ter Horst GJ, van Der Vliet J, and Buijs RM**. Physiological and anatomic evidence for regulation of the heart by suprachiasmatic nucleus in rats. *Am J Physiol Heart Circ Physiol* 280: H1391-1399, 2001.

8. **Schroder EA, Burgess DE, Zhang X, Lefta M, Smith JL, Patwardhan A, Bartos DC, Elayi CS, Esser KA, and Delisle BP**. The cardiomyocyte molecular clock regulates the circadian expression of Kcnh2 and contributes to ventricular repolarization. *Heart Rhythm* 12: 1306-1314, 2015.

9. **Gottlieb LA, Larsen K, Halade GV, Young ME, and Thomsen MB**. Prolonged QT intervals in mice with cardiomyocyte-specific deficiency of the molecular clock. *Acta Physiol (Oxf)* 233: e13707, 2021.

10. **Delisle BP, Stumpf JL, Wayland JL, Johnson SR, Ono M, Hall D, Burgess DE, and Schroder EA**. Circadian clocks regulate cardiac arrhythmia susceptibility, repolarization, and ion channels. *Curr Opin Pharmacol* 57: 13-20, 2021.

11. **D'Souza A, Wang Y, Anderson C, Bucchi A, Baruscotti M, Olieslagers S, Mesirca P, Johnsen AB, Mastitskaya S, Ni H, Zhang Y, Black N, Cox C, Wegner S, Bano-Otalora B, Petit C, Gill E, Logantha S, Dobrzynski H, Ashton N, Hart G, Zhang R, Zhang H, Cartwright EJ, Wisloff U, Mangoni ME, da Costa Martins PA, Piggins HD, DiFrancesco D, and Boyett MR**. A circadian clock in the sinus node mediates day-night rhythms in Hcn4 and heart rate. *Heart Rhythm* 18: 801-810, 2021.

12. **Jeyaraj D, Haldar SM, Wan X, McCauley MD, Ripperger JA, Hu K, Lu Y, Eapen BL, Sharma N, Ficker E, Cutler MJ, Gulick J, Sanbe A, Robbins J, Demolombe S, Kondratov RV, Shea SA, Albrecht U, Wehrens XH, Rosenbaum DS, and Jain MK**. Circadian rhythms govern cardiac repolarization and arrhythmogenesis. *Nature* 483: 96-99, 2012.

13. **Schroder EA, Wayland JL, Samuels KM, Shah SF, Burgess DE, Seward T, Elayi CS, Esser KA, and Delisle BP**. Cardiomyocyte Deletion of Bmal1 Exacerbates QT- and RR-Interval Prolongation in Scn5a (+/ΔKPQ) Mice. *Front Physiol* 12: 681011, 2021.

14. **Schroder EA, Lefta M, Zhang X, Bartos DC, Feng HZ, Zhao Y, Patwardhan A, Jin JP, Esser KA, and Delisle BP**. The cardiomyocyte molecular clock, regulation of Scn5a, and arrhythmia susceptibility. *Am J Physiol Cell Physiol* 304: C954-965, 2013.

15. **Schroder EA, Burgess DE, Manning CL, Zhao Y, Moss AJ, Patwardhan A, Elayi CS, Esser KA, and Delisle BP**. Light phase-restricted feeding slows basal heart rate to exaggerate the type-3 long QT syndrome phenotype in mice. *Am J Physiol Heart Circ Physiol* 307: H1777-1785, 2014.

16. **Zhang D, Colson JC, Jin C, Becker BK, Rhoads MK, Pati P, Neder TH, King MA, Valcin JA, Tao B, Kasztan M, Paul JR, Bailey SM, Pollock JS, Gamble KL, and Pollock DM**. Timing of Food Intake Drives the Circadian Rhythm of Blood Pressure. *Function (Oxf)* 2: zqaa034, 2021.

17. **Damiola F, Le Minh N, Preitner N, Kornmann B, Fleury-Olela F, and Schibler U**. Restricted feeding uncouples circadian oscillators in peripheral tissues from the central pacemaker in the suprachiasmatic nucleus. *Genes Dev* 14: 2950-2961, 2000.

18. **Schroder EA, Burgess DE, Johnson SR, Ono M, Seward T, Elayi CS, Esser KA, and Delisle BP**. Timing of food intake in mice unmasks a role for the cardiomyocyte circadian clock mechanism in limiting QT-interval prolongation. *Chronobiol Int* 1-10, 2021.
19. **Clark AJ**. The effect of alterations of temperature upon the functions of the isolated heart. *J Physiol* 54: 275-286, 1920.
20. **Tanner JM**. The relationships between the frequency of the heart, oral temperature and rectal temperature in man at rest. *J Physiol* 115: 391-409, 1951.
21. **Kirschen GW, Singer DD, Thode HC, Jr., and Singer AJ**. Relationship between body temperature and heart rate in adults and children: A local and national study. *Am J Emerg Med* 38: 929-933, 2020.
22. **Swoap SJ, and Gutilla MJ**. Cardiovascular changes during daily torpor in the laboratory mouse. *Am J Physiol Regul Integr Comp Physiol* 297: R769-774, 2009.
23. **Wu Y, Wang Q, Granger J, Gaido OR, Aguilar EN, Ludwig A, Moroni A, Bianchet MA, and Anderson ME**. HCN channels sense temperature and determine heart rate responses to heat. *bioRxiv* 2023.
24. **Fleming PR, and Muir FH**. Electrocardiographic changes in induced hypothermia in man. *Br Heart J* 19: 59-66, 1957.
25. **Hicks CE, McCord MC, and Blount SG, Jr.** Electrocardiographic changes during hypothermia and circulatory occlusion. *Circulation* 13: 21-28, 1956.
26. **Karjalainen J, and Viitasalo M**. Fever and cardiac rhythm. *Arch Intern Med* 146: 1169-1171, 1986.
27. **Mattu A, Brady WJ, and Perron AD**. Electrocardiographic manifestations of hypothermia. *Am J Emerg Med* 20: 314-326, 2002.
28. **Yaganti VM, Naik CA, and Dhond AJ**. Electrocardiographic manifestations in a hypothermic patient: review of Osborn waves. *Indian Heart J* 59: 80-82, 2007.
29. **van der Linde HJ, Van Deuren B, Teisman A, Towart R, and Gallacher DJ**. The effect of changes in core body temperature on the QT interval in beagle dogs: a previously ignored phenomenon, with a method for correction. *Br J Pharmacol* 154: 1474-1481, 2008.
30. **Schibler U, Gotic I, Saini C, Gos P, Curie T, Emmenegger Y, Sinturel F, Gosselin P, Gerber A, Fleury-Olela F, Rando G, Demarque M, and Franken P**. Clock-Talk: Interactions between Central and Peripheral Circadian Oscillators in Mammals. *Cold Spring Harb Symp Quant Biol* 80: 223-232, 2015.
31. **Guzadhur L, Pearcey SM, Duehmke RM, Jeevaratnam K, Hohmann AF, Zhang Y, Grace AA, Lei M, and Huang CL**. Atrial arrhythmogenicity in aged Scn5a+/DeltaKPQ mice modeling long QT type 3 syndrome and its relationship to Na+ channel expression and cardiac conduction. *Pflugers Arch* 460: 593-601, 2010.
32. **Zhang Y, Wu J, King JH, Huang CL, and Fraser JA**. Measurement and interpretation of electrocardiographic QT intervals in murine hearts. *Am J Physiol Heart Circ Physiol* 306: H1553-1557, 2014.
33. **Nuyens D, Stengl M, Dugarmaa S, Rossenbacker T, Compernolle V, Rudy Y, Smits JF, Flameng W, Clancy CE, Moons L, Vos MA, Dewerchin M, Benndorf K, Collen D, Carmeliet E, and Carmeliet P**. Abrupt rate accelerations or premature beats cause life-threatening arrhythmias in mice with long-QT3 syndrome. *Nature Medicine* 7: 1021-1027, 2001.

34. **Skop V, Guo J, Liu N, Xiao C, Hall KD, Gavrilova O, and Reitman ML**. Mouse Thermoregulation: Introducing the Concept of the Thermoneutral Point. *Cell Rep* 31: 107501, 2020.
35. **Lund K, Nygaard H, and Kirstein Pedersen A**. Weighing the QT intervals with the slope or the amplitude of the T wave. *Ann Noninvasive Electrocardiol* 7: 4-9, 2002.
36. **Hughes ME, Hogenesch JB, and Kornacker K**. JTK_CYCLE: an efficient nonparametric algorithm for detecting rhythmic components in genome-scale data sets. *J Biol Rhythms* 25: 372-380, 2010.
37. **Bray MS, Ratcliffe WF, Grenett MH, Brewer RA, Gamble KL, and Young ME**. Quantitative analysis of light-phase restricted feeding reveals metabolic dyssynchrony in mice. *Int J Obes (Lond)* 37: 843-852, 2013.
38. **Satoh Y, Kawai H, Kudo N, Kawashima Y, and Mitsumoto A**. Time-restricted feeding entrains daily rhythms of energy metabolism in mice. *Am J Physiol Regul Integr Comp Physiol* 290: R1276-1283, 2006.
39. **Barazi N, Polidovitch N, Debi R, Yakobov S, Lakin R, and Backx PH**. Dissecting the Roles of the Autonomic Nervous System and Physical Activity on Circadian Heart Rate Fluctuations in Mice. *Front Physiol* 12: 692247, 2021.
40. **Gordan R, Gwathmey JK, and Xie LH**. Autonomic and endocrine control of cardiovascular function. *World J Cardiol* 7: 204-214, 2015.
41. **Fenske S, Probstle R, Auer F, Hassan S, Marks V, Pauza DH, Biel M, and Wahl-Schott C**. Comprehensive multilevel in vivo and in vitro analysis of heart rate fluctuations in mice by ECG telemetry and electrophysiology. *Nat Protoc* 11: 61-86, 2016.
42. **Goldstein DS, Bentho O, Park MY, and Sharabi Y**. Low-frequency power of heart rate variability is not a measure of cardiac sympathetic tone but may be a measure of modulation of cardiac autonomic outflows by baroreflexes. *Exp Physiol* 96: 1255-1261, 2011.
43. **Press WH, and Numerical Recipes Software (Firm)**. Numerical recipes in C. Cambridge, England ; New York, N.Y.: Cambridge University Press,, 1992, p. 1 computer disk 5 1/4 in.
44. **Levine JD, Funes P, Dowse HB, and Hall JC**. Signal analysis of behavioral and molecular cycles. *BMC Neurosci* 3: 1, 2002.
45. **Team Rc**. R: A Language and Environment for Statistical Computing R Foundation for Statistical Computing. https://www.R-project.org.
46. **Rose RA, Kabir MG, and Backx PH**. Altered heart rate and sinoatrial node function in mice lacking the cAMP regulator phosphoinositide 3-kinase-gamma. *Circ Res* 101: 1274-1282, 2007.
47. **Krishnaswamy PS, Egom EE, Moghtadaei M, Jansen HJ, Azer J, Bogachev O, Mackasey M, Robbins C, and Rose RA**. Altered parasympathetic nervous system regulation of the sinoatrial node in Akita diabetic mice. *J Mol Cell Cardiol* 82: 125-135, 2015.
48. **Egom EE, Vella K, Hua R, Jansen HJ, Moghtadaei M, Polina I, Bogachev O, Hurnik R, Mackasey M, Rafferty S, Ray G, and Rose RA**. Impaired sinoatrial node function and increased susceptibility to atrial fibrillation in mice lacking natriuretic peptide receptor C. *J Physiol* 593: 1127-1146, 2015.

49. **Mulla W, Murninkas M, Levi O, and Etzion Y**. Incorrectly corrected? QT interval analysis in rats and mice. *Front Physiol* 13: 1002203, 2022.
50. **Mulla W, Gillis R, Murninkas M, Klapper-Goldstein H, Gabay H, Mor M, Elyagon S, Liel-Cohen N, Bernus O, and Etzion Y**. Unanesthetized Rodents Demonstrate Insensitivity of QT Interval and Ventricular Refractory Period to Pacing Cycle Length. *Front Physiol* 9: 897, 2018.
51. **Ripplinger CM, Glukhov AV, Kay MW, Boukens BJ, Chiamvimonvat N, Delisle BP, Fabritz L, Hund TJ, Knollmann BC, Li N, Murray KT, Poelzing S, Quinn TA, Remme CA, Rentschler SL, Rose RA, and Posnack NG**. Guidelines for assessment of cardiac electrophysiology and arrhythmias in small animals. *Am J Physiol Heart Circ Physiol* 323: H1137-H1166, 2022.
52. **Swoap SJ, Li C, Wess J, Parsons AD, Williams TD, and Overton JM**. Vagal tone dominates autonomic control of mouse heart rate at thermoneutrality. *Am J Physiol Heart Circ Physiol* 294: H1581-1588, 2008.
53. **Scheer FA, Hilton MF, Mantzoros CS, and Shea SA**. Adverse metabolic and cardiovascular consequences of circadian misalignment. *Proc Natl Acad Sci U S A* 106: 4453-4458, 2009.
54. **Sano H, Hayashi H, Makino M, Takezawa H, Hirai M, Saito H, and Ebihara S**. Effects of suprachiasmatic lesions on circadian rhythms of blood pressure, heart rate and locomotor activity in the rat. *Jpn Circ J* 59: 565-573, 1995.
55. **Schroder EA, and Delisle BP**. Time Restricted Feeding to the Light Cycle Dissociates Canonical Circadian Clocks and Physiological Rhythms in Heart Rate. *Front Pharmacol* 13: 910195, 2022.
56. **Warren WS, Champney TH, and Cassone VM**. The suprachiasmatic nucleus controls the circadian rhythm of heart rate via the sympathetic nervous system. *Physiol Behav* 55: 1091-1099, 1994.
57. **Curtis AM, Cheng Y, Kapoor S, Reilly D, Price TS, and Fitzgerald GA**. Circadian variation of blood pressure and the vascular response to asynchronous stress. *Proc Natl Acad Sci U S A* 104: 3450-3455, 2007.
58. **Schroder EA, Ono M, Johnson SR, Rozmus ER, Burgess DE, Esser KA, and Delisle BP**. The role of the cardiomyocyte circadian clocks in ion channel regulation and cardiac electrophysiology. *J Physiol* 600: 2037-2048, 2022.
59. **Yang G, Chen L, Grant GR, Paschos G, Song WL, Musiek ES, Lee V, McLoughlin SC, Grosser T, Cotsarelis G, and FitzGerald GA**. Timing of expression of the core clock gene Bmal1 influences its effects on aging and survival. *Sci Transl Med* 8: 324ra316, 2016.
60. **Hayter EA, Wehrens SMT, Van Dongen HPA, Stangherlin A, Gaddameedhi S, Crooks E, Barron NJ, Venetucci LA, Neill JSO, Brown TM, Skene DJ, Trafford AW, and Bechtold DA**. Distinct circadian mechanisms govern cardiac rhythms and susceptibility to arrhythmia. *Nat Commun* 12: 2472, 2021.
61. **Refinetti R**. Circadian rhythmicity of body temperature and metabolism. *Temperature (Austin)* 7: 321-362, 2020.
62. **Postema PG, and Wilde AA**. The measurement of the QT interval. *Curr Cardiol Rev* 10: 287-294, 2014.

63. **Molnar J, Zhang F, Weiss J, Ehlert FA, and Rosenthal JE**. Diurnal pattern of QTc interval: how long is prolonged? Possible relation to circadian triggers of cardiovascular events. *J Am Coll Cardiol* 27: 76-83, 1996.
64. **Browne KF, Prystowsky E, Heger JJ, Chilson DA, and Zipes DP**. Prolongation of the Q-T interval in man during sleep. *Am J Cardiol* 52: 55-59, 1983.
65. **Gohari A, Wiebe D, and Ayas N**. Shift working and cardiovascular health. *Chronobiol Int* 40: 27-32, 2023.
66. **Sabir IN, Killeen MJ, Grace AA, and Huang CL**. Ventricular arrhythmogenesis: insights from murine models. *Prog Biophys Mol Biol* 98: 208-218, 2008.

Figure Legends

Figure 1. Light cycle-restricted feeding caused large changes in hourly RR intervals, QT intervals, PR intervals, and core body temperature. A. Representative ensemble ECG traces recorded from a mouse in ad libitum-fed conditions (ALF, left column), after initially starting light cycle-restricted feeding (L-RF_i, middle column), and two weeks after starting light cycle-restricted feeding (L-RF_{2wk}, right column) at different Zeitgeber times (ZT). **B.** Averaged time series data showing three consecutive days of the hourly mean for the RR interval (vermillion), QT interval (sky blue), PR interval (orange), and core body temperature (Tb, reddish purple). The data were plotted as a function of ZT and the shaded regions correspond to the dark cycle. The left column shows the data recorded during ALF, the middle column shows the data recorded during L-RF_i (the boxed arrow indicates 24 hours after the start of light cycle-restricted feeding), and the right column shows the data recorded after L-RF_{2wk}. The solid lines are cosine curves fitted to the data (n = 6 mice, data points are averaged data and SD).

Figure 2. Light cycle-restricted feeding modified the properties of the 24-hour rhythms for RR intervals, QT intervals, PR intervals, and core body temperature. The individual mouse time series data for the RR intervals, QT intervals, PR intervals, and core body temperature (Tb) were fit to a cosine wave to calculate the acrophase, amplitude, and mesor for mice in ad libitum-fed conditions (ALF), 24 hours after initially starting light cycle-restricted feeding (L-RF_i), and two weeks after starting light cycle-restricted feeding (L-RF_{2wk}). **See Supplemental Table 1. A.** The top row shows the acrophase of the RR interval (vermillion), QT interval (sky blue), PR interval (orange), and Tb (reddish purple) for each condition. **B.** The top row shows the amplitude, and the bottom row shows the mesor of the RR interval, QT interval, PR interval, and Tb for each condition. Data were analyzed using a two-way mixed effects model (**see Figure 3S**) with Geisser and Greenhouse correction and Sidăk correction, *$p<0.05$, **$p<0.01$, ***$p<0.001$, ****$p<0.0001$, n = 5-6 mice per group.

Figure 3. Light cycle-restricted feeding altered heart rate variability and activity. A. The top row of graphs shows the averaged time series data for three consecutive days of the hourly mean for the RR interval from **Figure 1** (grey) overlayed with the estimated $RR_{\text{core body temperature}}$ interval (green). The left column shows the data from mice in ad libitum-conditions (ALF), the middle column shows the data initially starting light cycle-restricted feeding (L-RF_i), and the third column shows the data two weeks after starting light cycle-restricted feeding (L-RF_{2wk}). The middle row of graphs shows the corresponding data for the power of the high-frequency component in heart rate variability (pHF, blue), and the bottom row of graphs shows the corresponding data for cage activity (yellow). Data were plotted as a function of ZT and the shaded regions correspond to the dark cycle (n = 6 mice, data points are averaged data and SD). **B.** The left graph shows the average pHF value for each mouse during the light cycle (open circle) and dark cycle (solid circle) measured during ALF, L-RF_i, and L-RF_{2wk}. The right graph shows the average activity value for each mouse during the light cycle (open circle) and dark cycle (solid circle) during ALF, L-RF_i, and L-RF_{2wk}. Data were analyzed

using a one-way ANOVA with Geisser and Greenhouse correction and Sidăk correction, *p<0.05 and **p<0.01, n = 6 mice per group.

Figure 4. After starting light cycle-restricted feeding, the RR interval continued to show correlated rhythmicity with core body temperature and pHF but not activity. The mean data and SD for the cross-correlation between the time series data for the RR interval and core body temperature (Tb, top row, reddish purple), power of the high-frequency component in heart rate variability (pHF, middle row, blue), and activity (bottom row, yellow) in ad libitum-fed conditions (ALF, left column), after initially starting light cycle-restricted feeding (L-RF_i, middle column), and two weeks after starting light cycle-restricted feeding (L-RF_{2wk}, right column). The peak correlation coefficient at lag 0 is shown (n = 6 mice per group). Differences in the peak correlation coefficient data at lag 0 were analyzed using a one-way ANOVA with Geisser and Greenhouse correction and Sidăk correction *p<0.05 and **p<0.01.

Figure 5. Inhibition of autonomic receptor activation caused a loss in the daily rhythm of the RR interval during light cycle-restricted feeding. A. Time series data showing the hourly mean in the RR interval (vermillion) and core body temperature (Tb, reddish purple) recorded 1 week after the start of light cycle-restricted feeding (ZT 3 to ZT 9). The data were plotted as a function of ZT and the shaded regions represent the dark cycle. The time series shows the hourly mean data and SD measured during the light and dark cycle the day before starting the propranolol and atropine injections (LC0, DC0), and the first and second light and dark cycles after starting the propranolol and atropine injections at ZT 23.5 and ZT 9.5 (LC1, DC1, LC2, and DC2, respectively, injection times are denoted by arrows; n = 5 mice). **B.** Shown are the RR interval (vermillion) and Tb (reddish purple) data recorded during LC0 and DC0, LC1 and DC1, and LC2 and DC2; the horizontal bar in each data set is the mean data. The data were analyzed using a two-way ANOVA with Geisser and Greenhouse correction and Tukey correction, *p<0.05, **p<0.01, ***p<0.001. **C.** Time series of RR interval data from **A.** overlayed with the averaged time series for the corresponding $RR_{\text{core body temperature}}$ interval (blue) before and after injection with propranolol and atropine.

Figure 6. Correcting the QT interval for core body temperature caused a loss in the daily rhythm in the QT interval. A. The left graph shows the hourly mean in the QT interval plotted as a function of the corresponding core body temperature (Tb) for each mouse in ad libitum-fed conditions, initially after starting light cycle-restricted feeding, and two weeks after starting light cycle-restricted feeding (each mouse is represented by a different color, n = 6). The average slope was used to correct the QT interval to 37°C ($QT_{37°C}$ interval). The right graph shows the $QT_{37°C}$ interval is plotted as a function of the corresponding Tb for the same set of mice. Linear regression of the data for each mouse (red lines) was used to calculate the average slope and R^2 and SD for both the left and right graphs. **B.** The left column shows the hourly $QT_{37°C}$ interval and SD calculated during ad libitum-fed conditions (ALF), the middle column shows the $QT_{37°C}$ interval initially starting light cycle-restricted feeding (L-RF_i), and the third column shows the $QT_{37°C}$ interval two weeks after starting light cycle-restricted feeding (L-RF_{2wk}). Also shown is the corresponding time series data for the hourly mean in the

uncorrected QT interval data from **Figure 1** for direct comparison (grey). Data were plotted as a function of ZT and the shaded regions represent the dark cycle.

Figure 7. Housing mice in thermoneutrality unmasked distinct mechanisms regulating daily rhythms in RR and QT intervals. A. Representative hourly ensemble ECG traces recorded from a mouse in thermoneutrality at ZT 4 and 17. Also shown are the time series data for the hourly mean (and SD) for the RR (sky blue), $RR_{\text{core body temperature}}$ (blue), QT (purple), and $QT_{37°C}$ (vermillion) intervals measured from mice in ad libitum-fed conditions housed at thermoneutrality. Data were plotted as a function of ZT and the shaded regions correspond to the dark cycle (n = 6 mice). **B.** The top graph plots the $QT_{37°C}$ interval as a function of the corresponding core body temperature (Tb) for the same set of mice in **A**. Each mouse is represented by a different color. The bottom graph shows the hourly mean in the uncorrected QT interval plotted as a function of the corresponding Tb. Linear regression (red lines) analysis for each mouse was used to calculate the mean slope and R^2 (including SD) for both data sets.

Figure 8. QT interval correction for core body temperature unmasked QT interval prolongation in a mouse model of long QT syndrome. A. The left column shows the hourly $QT_{37°C}$ interval and SD calculated from *Scn5a*$^{+/\Delta KPQ}$ mice (blue) during ad libitum-fed conditions (ALF), the middle column shows the $QT_{37°C}$ interval measured initially after starting light cycle-restricted feeding (L-RF_i), and the third column shows the $QT_{37°C}$ interval measured two weeks after starting light cycle-restricted feeding (L-RF_{2wk}). The graph also shows the mean hourly $QT_{37°C}$ interval measured from WT mice from **Figure 6** for comparison (grey) **C.** The graph shows $QT_{37°C}$ intervals measured from WT (grey) or *Scn5a*$^{+/\Delta KPQ}$ mice (blue) in ALF, L-RF_i, and L-RF_{2wk}. The horizontal bar in each data set is the mean (Data were analyzed using a two-way ANOVA with Geisser and Greenhouse correction and Sidăk correction, n = 6, *p<0.05,).

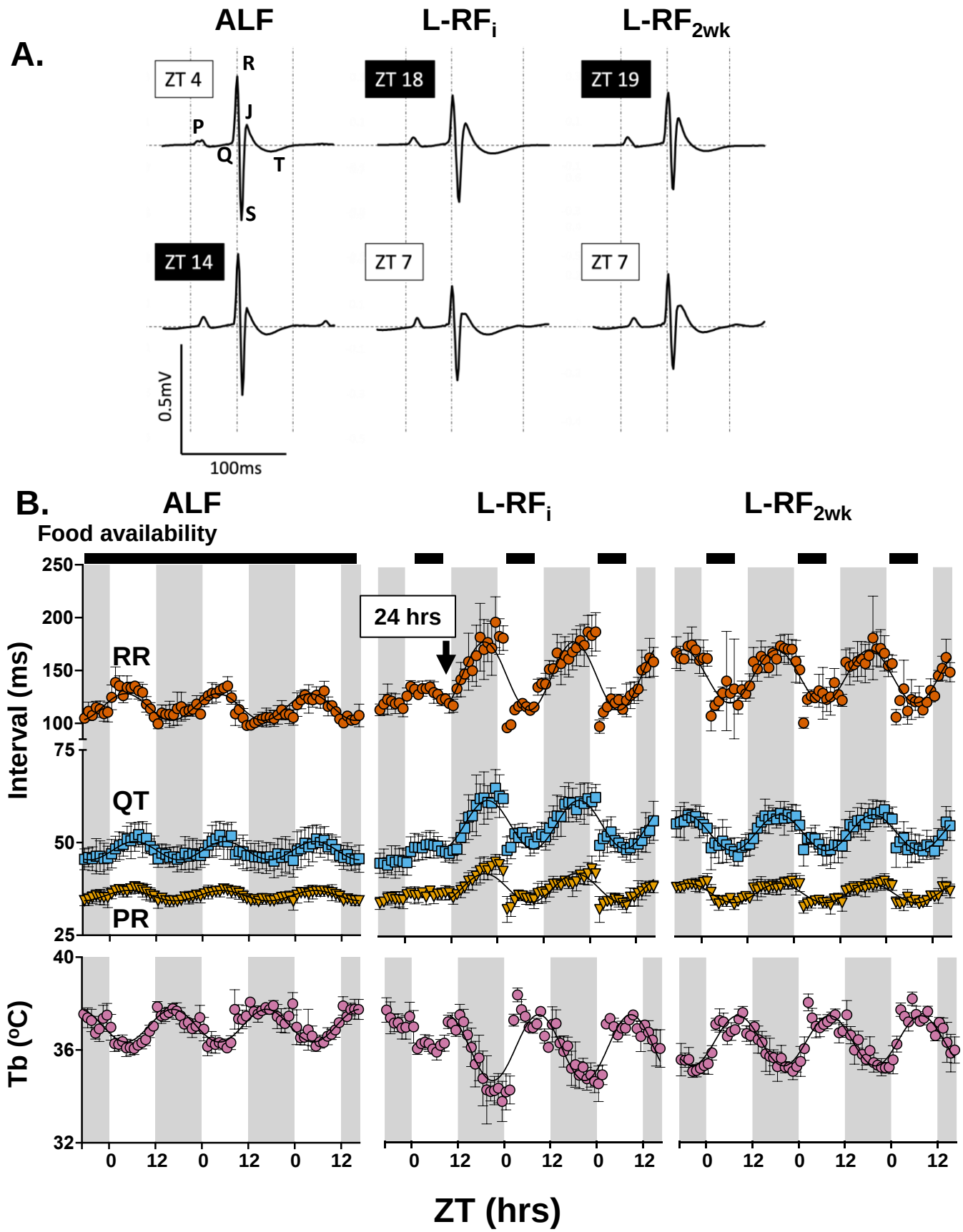
A.
ALF
L-RF$_i$
L-RF$_{2wk}$
ZT 4
ZT 18
ZT 19
ZT 14
ZT 7
ZT 7
R
J
P
Q
T
S
0.5mV
100ms
B.
ALF
L-RF$_i$
L-RF$_{2wk}$
Food availability
24 hrs
RR
QT
PR
Interval (ms)
Tb (ºC)
ZT (hrs)

Figure 1.

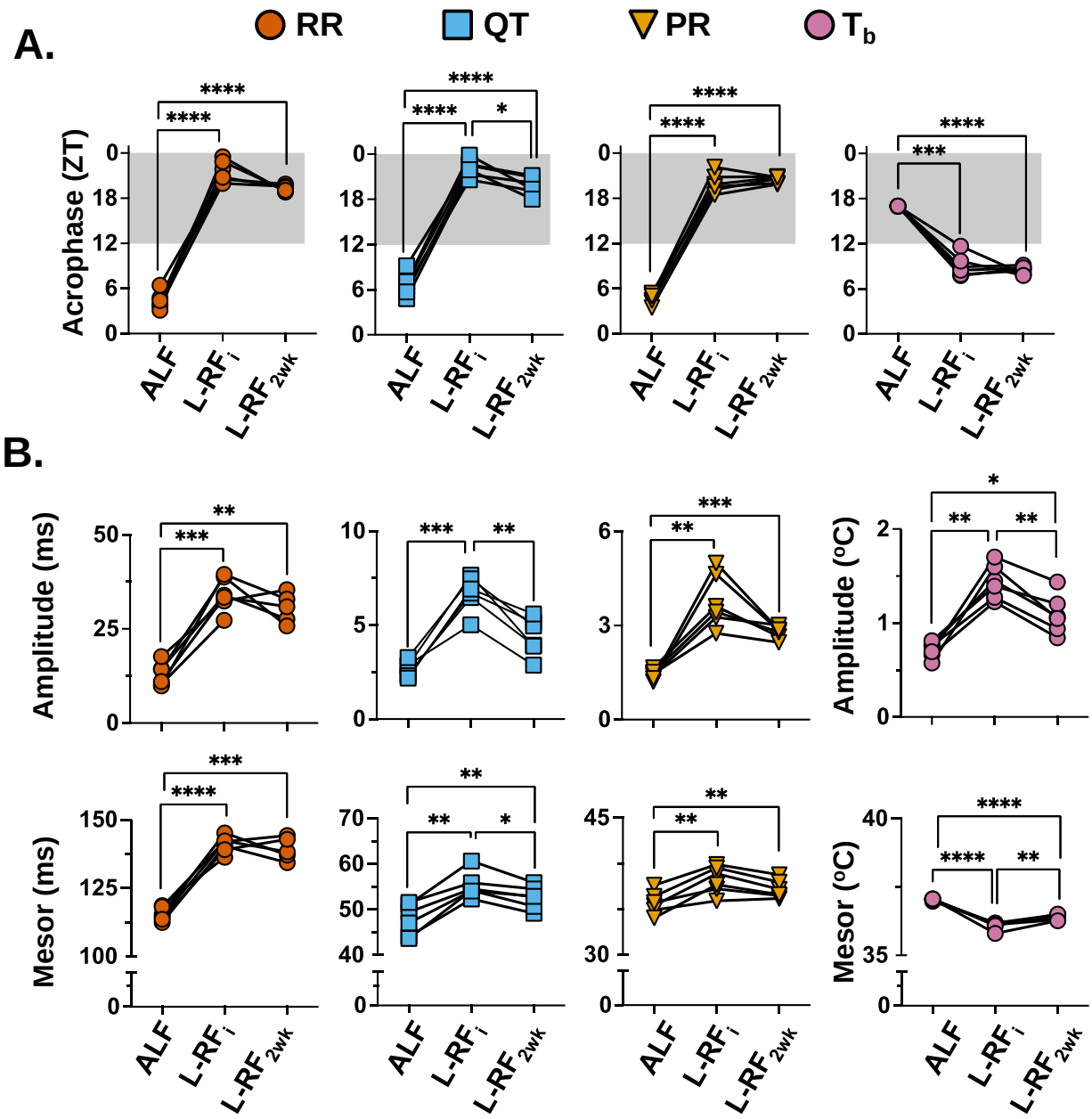
A.
RR
QT
PR
T_b
Acrophase (ZT)
B.
Amplitude (ms)
Amplitude (ºC)
Mesor (ms)
Mesor (ºC)
ALF
L-RF$_i$
L-RF$_{2wk}$

Figure 2.

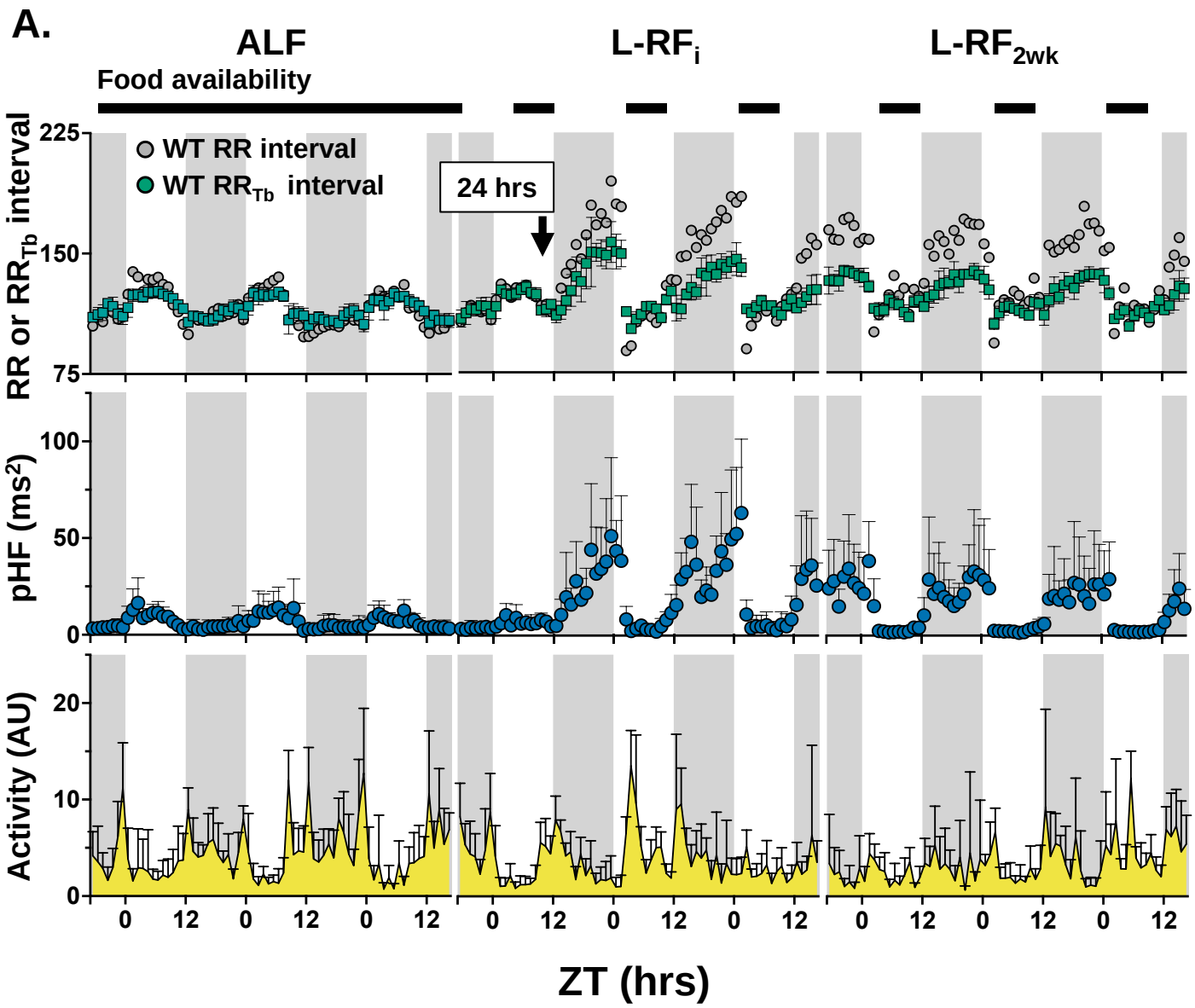
A.
ALF
L-RF$_i$
L-RF$_{2wk}$
Food availability
WT RR interval
WT RR$_{Tb}$ interval
24 hrs
RR or RR$_{Tb}$ interval
225
150
75
pHF (ms^2)
100
50
0
Activity (AU)
20
10
0
0
12
ZT (hrs)

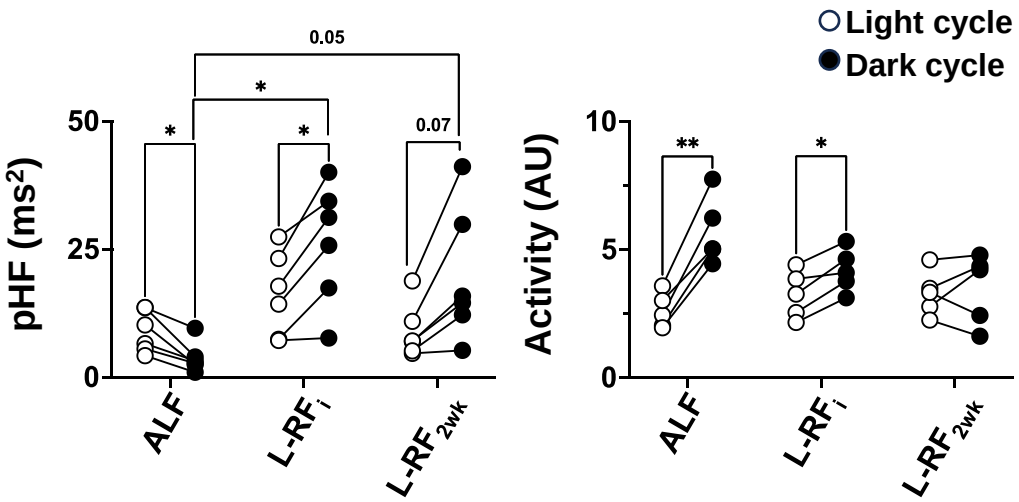
B.
Light cycle
Dark cycle
0.05
*
*
*
0.07
pHF (ms^2)
50
25
0
Activity (AU)
10
5
0
**
*
ALF
L-RF$_i$
L-RF$_{2wk}$

Figure 3.

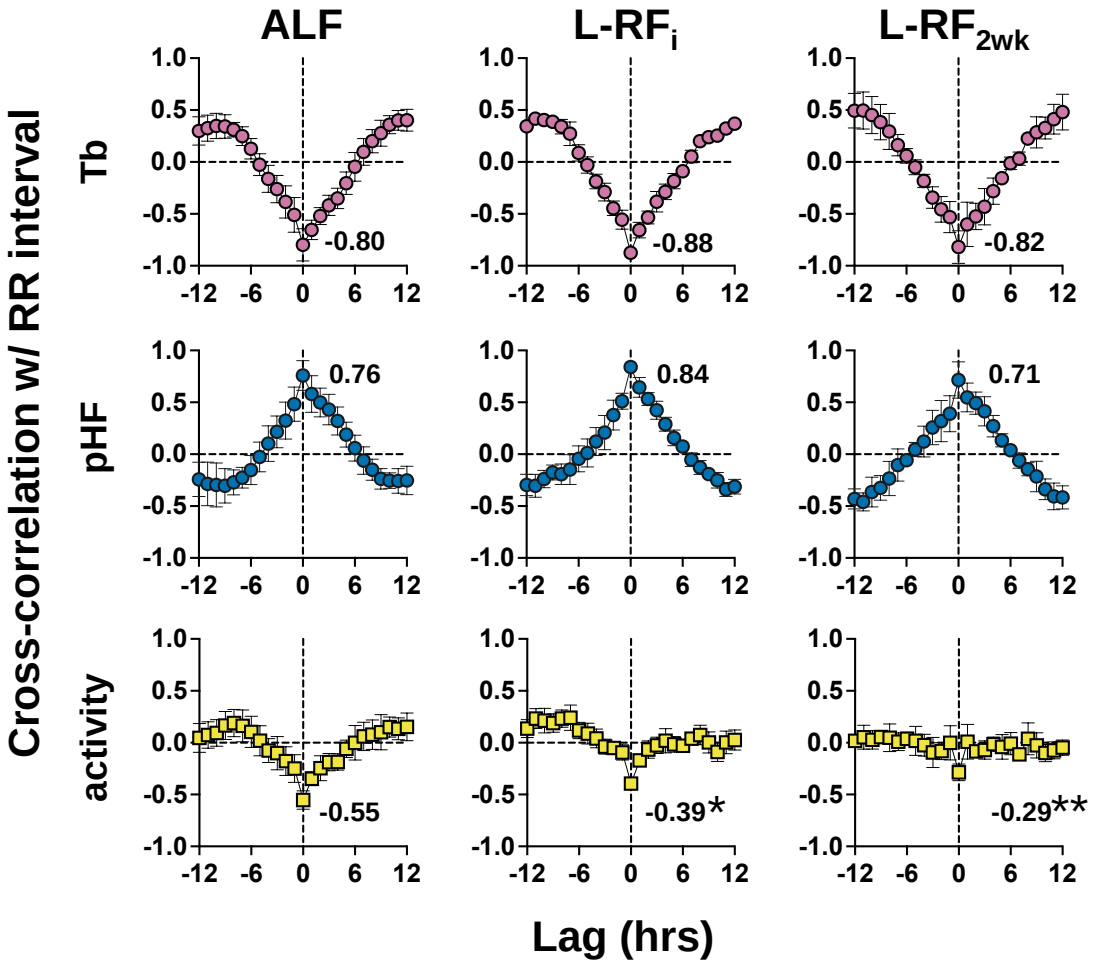
ALF
L-RF$_i$
L-RF$_{2wk}$
Tb
pHF
activity
Cross-correlation w/ RR interval
-0.80
-0.88
-0.82
0.76
0.84
0.71
-0.55
-0.39*
-0.29**
1.0
0.5
0.0
-0.5
-1.0
-12
-6
0
6
12
Lag (hrs)

Figure 4.

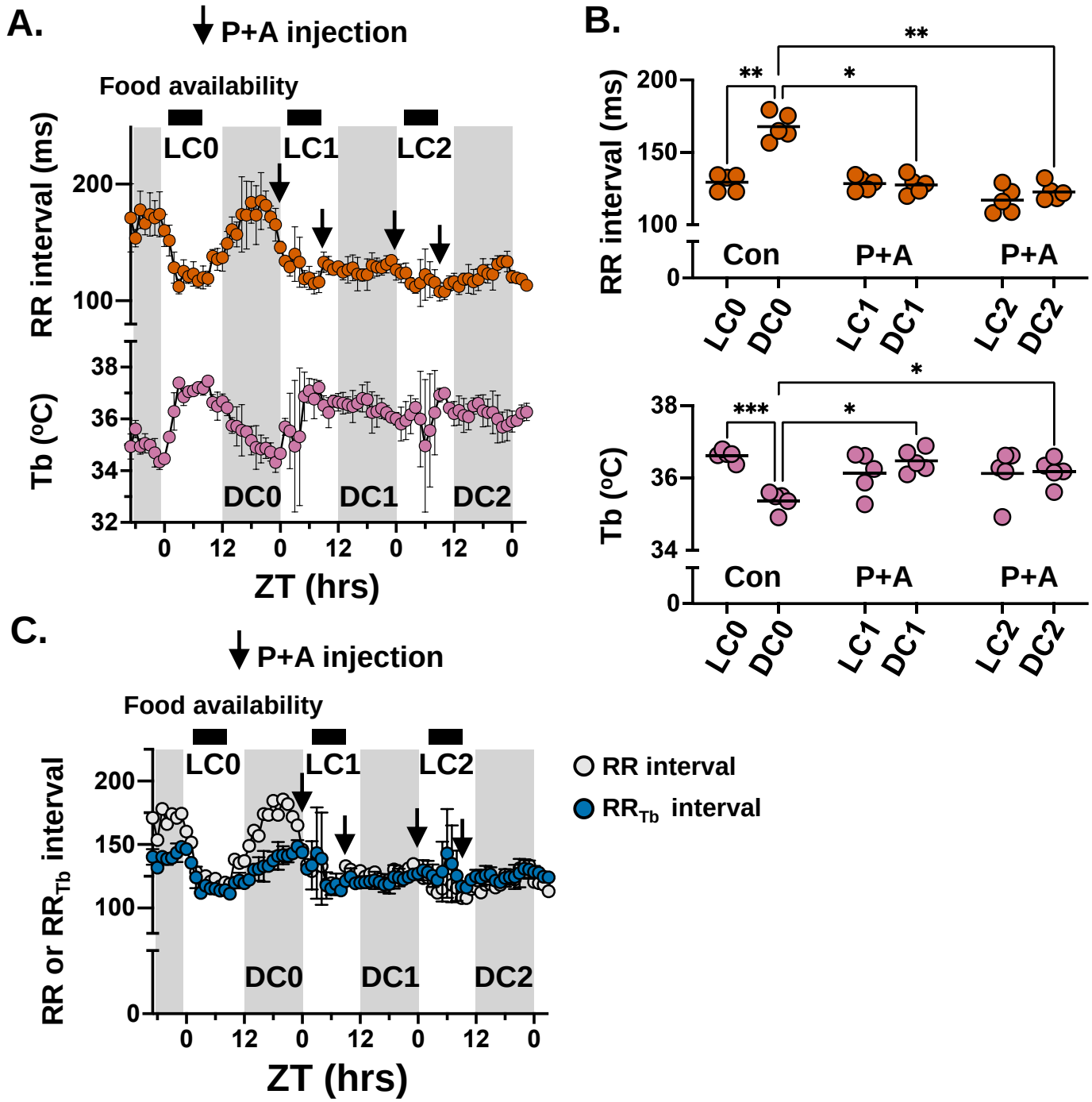
A.
P+A injection
Food availability
LC0
LC1
LC2
RR interval (ms)
200
100
Tb (ºC)
38
36
34
32
DC0
DC1
DC2
0
12
0
12
0
12
0
ZT (hrs)
B.
**
**
*
RR interval (ms)
200
150
100
0
Con
P+A
P+A
LC0
DC0
LC1
DC1
LC2
DC2
*
***
*
Tb (ºC)
38
36
34
0
Con
P+A
P+A
LC0
DC0
LC1
DC1
LC2
DC2
C.
P+A injection
Food availability
LC0
LC1
LC2
RR or RR$_{Tb}$ interval
200
150
100
0
DC0
DC1
DC2
0
12
0
12
0
12
0
ZT (hrs)
RR interval
RR$_{Tb}$ interval

Figure 5.

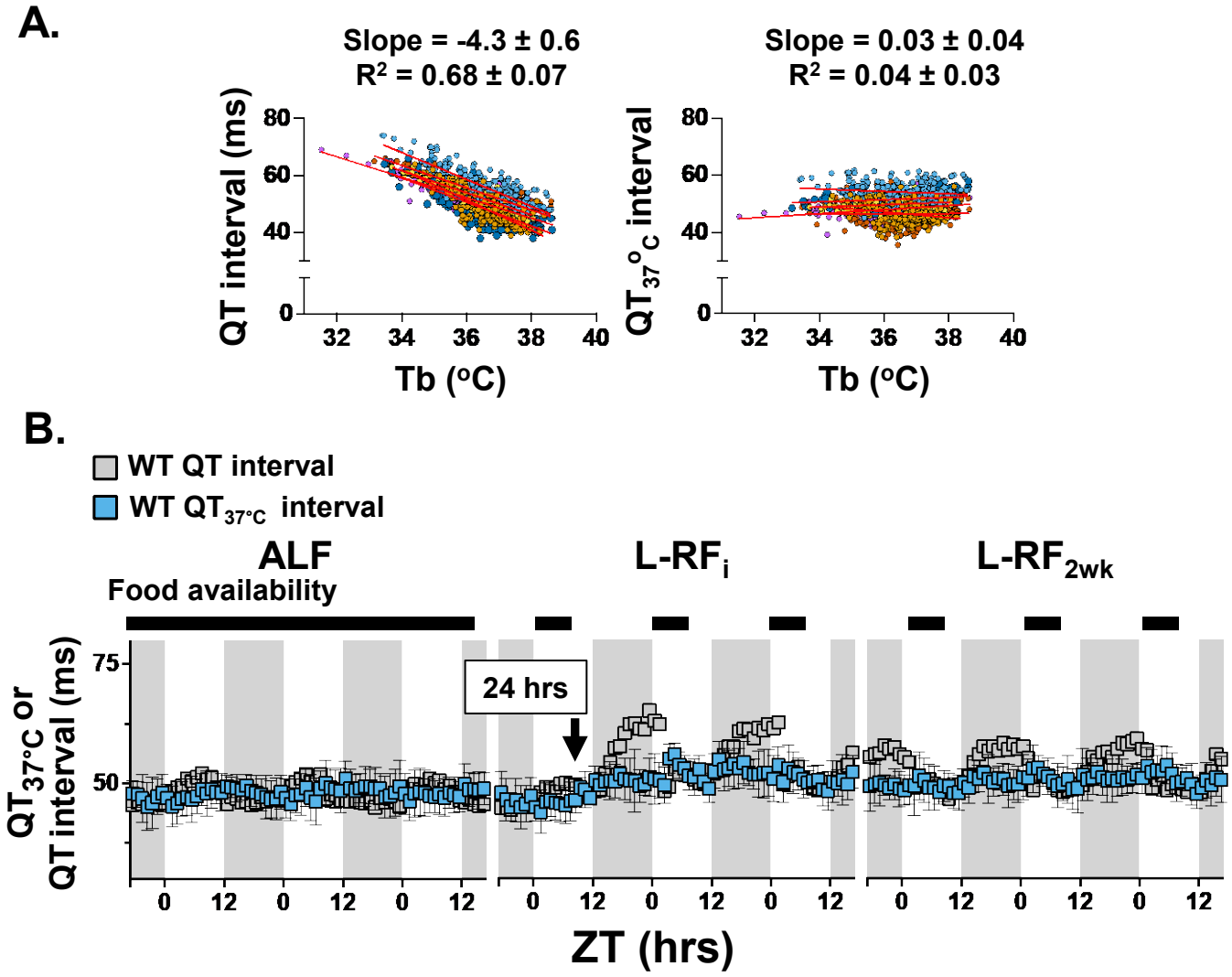
A.
Slope = -4.3 ± 0.6
R2 = 0.68 ± 0.07
QT interval (ms)
Tb (oC)
Slope = 0.03 ± 0.04
R2 = 0.04 ± 0.03
QT37oC interval
Tb (oC)
B.
WT QT interval
WT QT37°C interval
ALF
Food availability
L-RFi
L-RF2wk
24 hrs
QT37°C or QT interval (ms)
ZT (hrs)

Figure 6.

WT housed at 30ºC

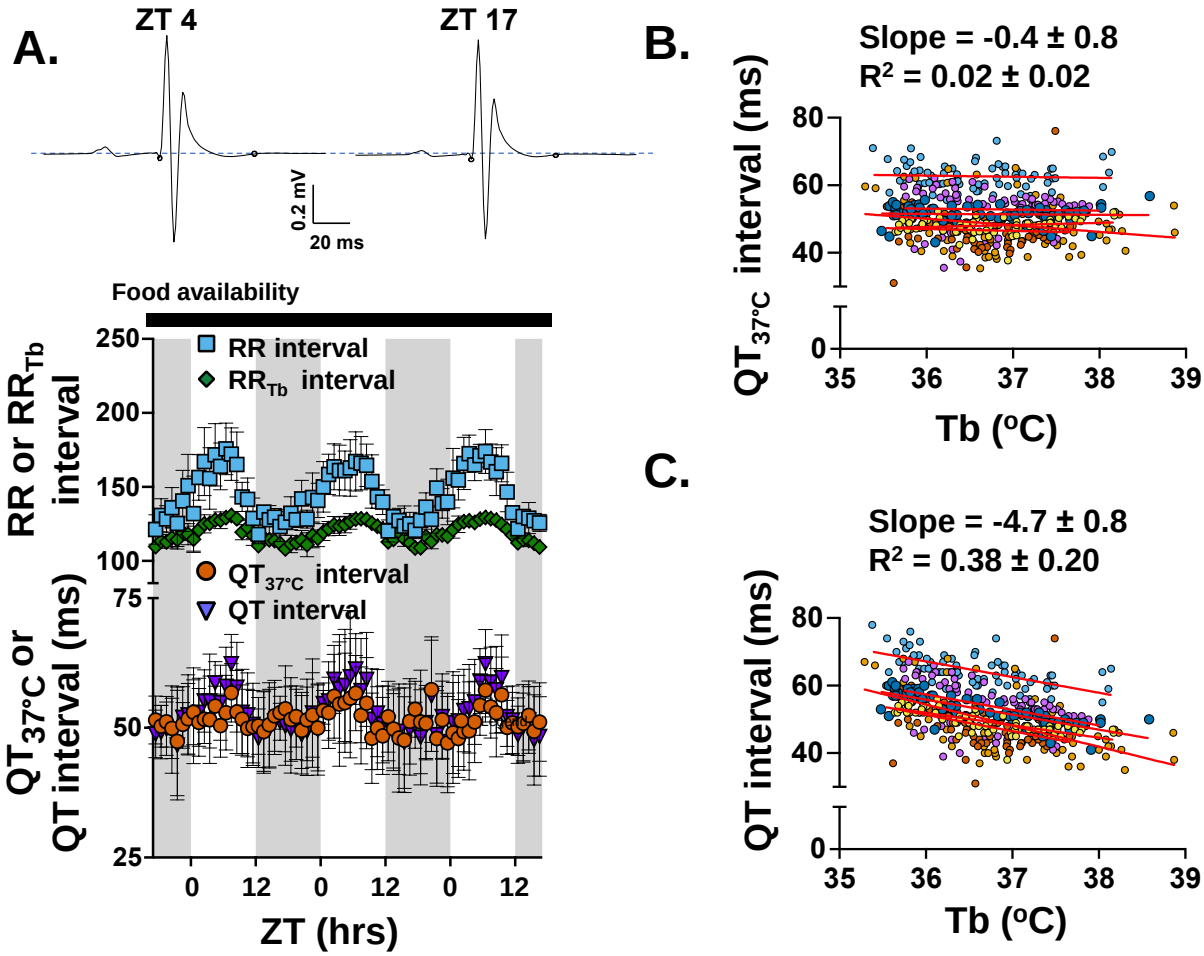

Figure 7.

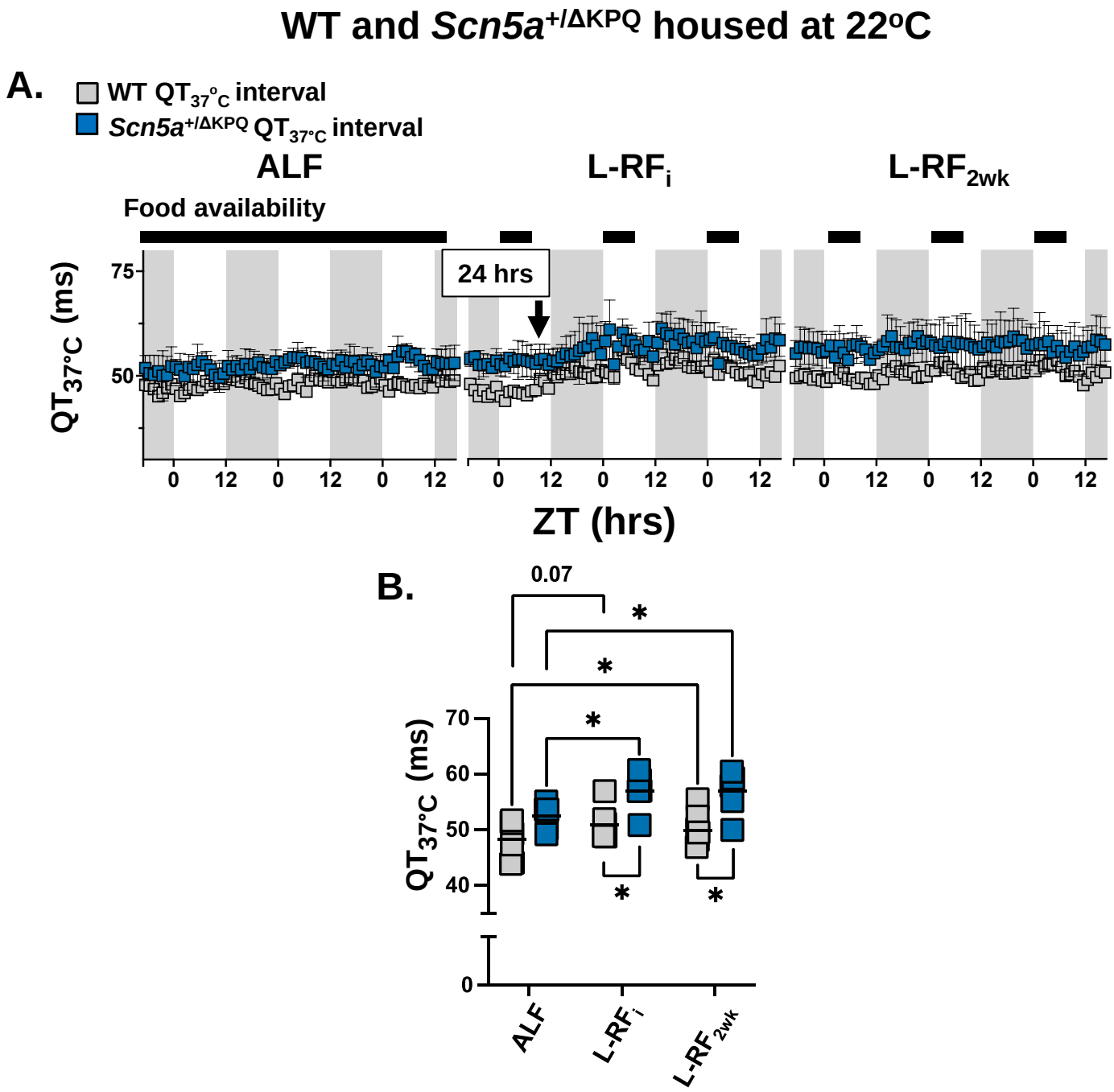
WT and Scn5a+/ΔKPQ housed at 22°C
A.
WT QT37°C interval
Scn5a+/ΔKPQ QT37°C interval
ALF
L-RFi
L-RF2wk
Food availability
24 hrs
QT37°C (ms)
75
50
0
12
ZT (hrs)
B.
0.07
*
70
60
40
ALF
L-RFi
L-RF2wk

Figure 8.